2022-08-25

Performance of deep-sea habitat suitability models assessed using independent data, and implications for use in area-based management

Howell, Kerry

10.3354/meps14098
Marine Ecology Progress Series
Inter Research

Performance of deep-sea habitat suitability models assessed using independent data, and implications for use in area-based management.

Kerry L. Howell[1*], Amelia E Bridges[1], Kyran P. Graves[1], Louise Allcock[2], Giulia la Bianca[1], Carolina Ventura-Costa[3], Sophie Donaldson[1], Anna-Leena Downie[4], Thomas Furey[5], Fergal McGrath[5], Rebecca Ross[6].

1. School of Biological and Marine Science, Plymouth University, Plymouth. PL4 8AA. UK

2. Ryan Institute and School of Natural Sciences, National University of Ireland Galway, Galway, Ireland.

3. University of Aveiro, Aveiro, Portugal

4. Centre for Environment, Fisheries and Aquaculture Science, Lowestoft, Suffolk. NR33 0HT. U.K.

5. Marine Institute, Rinville, Oranmore, Co. Galway. H91 R673

6. Institute of Marine Research, Bergen, Norway.

* Corresponding author email: kerry.howell@plymouth.ac.uk

Running page head: Performance of deep-sea habitat suitability models

Abstract

Marine spatial management requires accurate data on species and habitat distributions. In the deep sea, these data are lacking. Habitat suitability modelling offers a robust defensible means to fill data gaps, provided models are sufficiently reliable. We test the performance of published models of two deep-sea habitat-forming taxa at low and high resolutions (~1 km and 200 m grid-cell size), across the extended EEZs of UK and Ireland. We construct new data-rich models and compare new and old estimates of the area of habitat protected, noting changes in the protected area network since 2015. Results of independent validation suggest all published models perform worse than expected considering original cross-validation results, but model performance is still good or fair for *Desmophyllum pertusum* reef, with poorer performance for *Pheronema carpenteri* sponge models. High-resolution models using multibeam data out-perform low-resolution GEBCO-based models. Newly constructed models are good to excellent according to cross-validation. New model spatial predictions reflect published models, but with a significant reduction in predicted extent. The current marine protected area network and the European Union ban on bottom trawling below 800m protect 40% and 60% of *D. pertusum* reef-suitable habitat respectively, and 11% and 100% of *P. carpenteri* suitable habitat respectively within the model domain. We conclude high-resolution models of *D. pertusum* reef distribution are a useful tool in spatial management. The poorer performing *P. carpenteri* model indicate areas for more detailed study. Whilst low-resolution models can provide conservative estimates of percentage area-based conservation targets following the precautionary principle, high-resolution sea-floor mapping supports the development of better-performing models.

Key words: Deep sea; habitat suitability modelling; species distribution modelling; marine conservation; marine spatial planning

1. INTRODUCTION

As we begin the UN Decade of Ocean Science for Sustainable Development, the call for more holistic management of the marine environment is clear. Marine spatial planning (MSP) is an important tool supporting implementation of the 'ecosystem approach' to environmental management. An approach outlined in the Convention on Biological Diversity (CBD), and enshrined in the UN Sustainable Development Goals (UN General Assembly 2015). Maps lie at the heart of spatial management including maps of human uses, socio-economics, political and legal arrangements, and critically biophysical conditions and assemblages or communities of marine organisms, such as kelp forests and coral reefs. There is a pressing need to develop reliable accurate maps of the spatial distribution of marine ecosystems to support conservation initiatives.

Efforts to map benthic marine communities have largely focused on shallow water environments (Andrefouet et al. 2006, Traganos et al. 2018). Mapping deep-water communities is much more difficult because there is no direct equivalent to optical remote sensing which provides wide coverage of high-resolution data with direct observation of terrestrial and shallow (<10m) coastal habitats. The majority of deep-water benthic biological mapping has been achieved using modelling approaches. Species distribution modelling, also called habitat suitability modelling, uses data on the presence, absence, abundance or biomass of a species, assemblage or community, and relevant environmental data, to produce a statistical model of the relationship between species and their environmental drivers. The model can be used to make predictions of the distribution of the target species/community based on environmental data alone (Bryan & Metaxas 2007, Rengstorf et al. 2014, Howell et al. 2016). This type of mapping lends itself well to use in the marine environment as the

physical environment is often cheaper and simpler to measure than the biological components. There are a wealth of local, regional and global physical spatial models of the marine environment including oceanographic, bathymetric and productivity models. Benthic biological data are generally available for coastal marine areas and together with physical environmental data, offer great potential to produce relatively data-rich modelled maps. However, availability of benthic biological data decreases as you move away from the coast and into the deep sea (Webb et al. 2010), and this can present challenges in the development of reliable models.

The deep sea is increasingly subject to human use and there is an urgent need to implement more effective, integrated management of deep-sea ecosystems, through use of area-based management tools and marine spatial planning. The last 15 years has seen a growing trend in the use of predictive mapping techniques to generate models of the distribution of key species and assemblages in the deep sea (e.g. Bryan & Metaxas 2007, Guinan et al. 2009, Howell et al. 2011, Rengstorf et al. 2014, Robert et al. 2016, Howell et al. 2016, Pearman et al. 2020). These efforts have focused particularly on those species and assemblages that appear in key marine conservation legislation, and have produced modelled maps from a wide range of regions, of different extents and spatial resolutions. Models that provide large spatial coverage of a scale useful to national and regional MSP efforts, tend to use low-resolution (>1 km^2) modelled global environmental datasets in their production (Howell et al. 2016). Higher-resolution environmental datasets, such as multibeam bathymetry, and regional or site-specific oceanographic models, tend to only be employed in the construction of models with a more limited spatial extent (Pearman et al. 2020), rendering them less useful for national and regional scale MSP, but still informative.

While the potential applications of modelled maps in MSP have been demonstrated (Ross & Howell 2013, Howell et al. 2016, Stirling et al. 2016, Rowden et al. 2017), models are not yet widely used despite their obvious potential (Marshall et al. 2014, Reiss et al. 2015). This contrasts with many other fields, for example fisheries and climate science, where models are routinely used to forecast future scenarios, and the results used to make management and policy decisions (Hilborn 2012, IPCC 2014). The reasons for this are not clear. Addison et al. (2013), in their review of common objections to the use of models in environmental decision-making, identify nine key objections that are symptoms of three fundamental issues: (1) misconceptions about the role of models in decision-making, (2) poor modelling practice and (3) a lack of effective communication and/or trust between modellers and decision-makers. Objections around modelling practice and outputs include issues with model accuracy and uncertainty. Model performance is usually tested using random subsampling from the full model build dataset, so called cross-validation. However, the lack of true independence between testing and training data sets, as well as spatial sorting bias is known to artificially inflate model performances (Veloz 2009, Hijmans 2012) leading to a phenomenon where many models appear to perform well yet provide very different spatial predictions (Piechaud et al 2015; Howell et al 2016). This may serve to compound concerns around model accuracy and uncertainty, and highlight the need for independent validation of model performance to help allay these concerns and encourage wider use of model output.

In the North East Atlantic habitat suitability models for scleractinian cold water coral reef and an aggregation forming deep-sea sponge *Pheronema carpenteri* have been developed for the continental shelf claim areas of the UK and Ireland (Ross & Howell 2013, Ross et al. 2015). *Desmophyllum pertusum* reef is widely recognised as a distinct biological community or 'biotope', and occurs as thickets, discrete reefs, and giant carbonate mounds up to 300 m

high and several km in diameter. Within this region reefs have been observed on Hatton, George Bligh and Rockall Banks, the Wyville-Thomson Ridge, and in Explorer and Dangaard Canyons (Howell 2010, Howell et al. 2010), the Porcupine Seabight (Foubert et al. 2005, Huvenne et al. 2005), Porcupine Bank (Kenyon et al. 1998), southern Rockall Bank (Mienis et al. 2006, Wienberg et al. 2008) and Outer Hebrides (Roberts et al. 2005) as well as further north and south (Wheeler et al. 2007). Observations occur over depths from ~120 m to ~1000 m, with most reported from 600-800 m. Reef structures are highly biodiverse (Roberts et al. 2006), and have an important role as essential fish habitat (Husebø et al. 2002, Auster 2005).

P. carpenteri is a small spherical glass sponge that occurs singularly or in dense aggregations, predominantly (but not exclusively) on fine sandy mud and mud substrata. Within UK and Irish waters, aggregations are a recognised biotope, and communities composed of this species have been described from 1250 m in the Porcupine Seabight (Rice et al. 1990), 1100 m in the Hatton-Rockall Basin (Hughes & Gage 2004, Howell et al. 2014), and from 1450 m on Goban Spur (Lavaleye et al. 2002), with historical records of additional aggregations from Ireland to Spain in 1000-2000 m water (Le Danois 1948) and in the Northern Rockall Trough (Wyville-Thomson 1874). Aggregations are associated with an increase in abundance and richness of macrofauna observed within spicule mats and sponge bodies (Rice et al. 1990, Bett & Rice 1992). Recent studies have suggested that known aggregations may be poorly connected (potentially isolated) (Ross et al. 2019) and experience a substantive impact from bottom trawl fishing (Vieira et al. 2020). From a policy perspective both *D. pertusum* reef and *P. carpenteri* aggregations are considered Vulnerable Marine Ecosystems (VME) under United Nations General Assembly Resolution 61/105, and as 'threatened and/or declining species and habitats' under the OSPAR Convention for the Protection of the Marine Environment of

136 the north-east Atlantic 1992. Understanding their distribution is therefore an important
137 component to the development of area-based management of the region.

138 The Ross & Howell (2013) models were constructed using global scale environmental data
139 layers and are at a resolution of ~1 km^2. The Ross et al. (2015) models were constructed using
140 high resolution multibeam datasets and are at a resolution of 200x200 m grid cell size. Both
141 models were produced using the same underlying presence / absence biological dataset for
142 each response variable , *D. pertusum* reef habitat and *P. carpenteri* species. All four models
143 performed well when tested using cross-validation methods, and in general high-resolution
144 models performed better than low resolution models according to threshold-dependent
145 evaluation. However, the spatial predictions and resulting maps derived from models of
146 different resolution were notably different. The aim of this study is to undertake independent
147 validation of these published models of VME distribution in the UK and Irish ECS claim areas,
148 in order to assess model performance and inform future use in MSP and conservation.
149 Specifically, we will 1) independently validate model performance using newly collected
150 independent data, 2) construct new relatively data-rich models using the same modelling
151 method as the prior publications, 3) quantify changes in predicted distributions and
152 assessments of percentage protection targets for each VME (VME indicator taxa in the case
153 of *P. carpenteri*) as a result of new models.

154

155 **2. MATERIALS & METHODS**

156 2.1. Site and Model Description

157 The study considers the full extent of the Irish, and a partial extent of the UK's extended
158 continental shelf claim area in the N E Atlantic (Fig 1). A network comprising three different
159 types of Marine Protected Area (MPA) exists in this area for the protection of deep-sea
160 habitats (Fig 1). These are Special Areas for Conservation, OSPAR MPAs and North East
161 Atlantic Fisheries Commission (NEAFC) closures to bottom trawling for the protection of
162 VMEs. While the sites do not constitute a coherently designed MPA network, they enable
163 illustration of the potential use of habitat maps in area-based management. In addition, there
164 is a ban on bottom trawling below 800 m in European and UK waters.

165 Ross & Howell (2013) and Ross et al. (2015) scleractinian reef models were predominantly
166 constructed using *Desmophyllum pertusum reef* presence / absence data. However, a small
167 number of presence points for *Solenosmilia variabilis* reef were also included in the models.
168 In our experience *S. variabilis* appears to occupy the same topographic niche as *D. pertusum*
169 but occurs in deeper water. Records included in the models were at the shallow end of their
170 distribution only. The resulting models largely predicted the niche of *D. pertusum* reef but
171 with a slightly deeper reach. This study evaluates and builds upon the original models using
172 new *D. pertusum* reef data alone with *S. variabilis* reef data omitted. Ross & Howell's (2013)
173 models are of resolution 750x750 m grid cell size, and cover the full extent of both Irish and
174 UK continental shelf limit. Ross et al. (2015) models are of resolution 200x200 m grid cell size
175 and cover the full extent of the Irish, and partial extent of the UK's continental shelf limit in
176 the N E Atlantic. Both studies used their models to assess progress towards percent protection
177 conservation targets, and reported between 20 – 29% of scleractinian reef suitable habitat
178 and 1.9-2.9% of *P. carpenteri* suitable habitat is within the MPA network.

179

2.2. Biological Data

New data for both *P. carpenteri* and *D. pertusum* reef were compiled from five research cruises to the northeast Atlantic: i) Eurofleets2 funded DeepMap cruise CE15011 (2015), with ROV Holland I; ii) NERC funded Deep Links JC136 (2016), with ROV ISIS; iii, iv, v) Sea Rovers RH17001 (2017), RH18002 (2018) and CE19015 (2019), jointly funded by the Irish Government and EU, with ROV Holland I. These research cruises were not conducted for the sole purpose of model validation, but this was a consideration in transect line planning for all cruises. Transect lines ranged from approximately 100m to 3.1 km, with an average length of 1.3 km. Collectively these research cruises provide a dataset consisting of 195 high definition ROV video transects spread across the study area (Fig 1). This collective dataset is referred to throughout as the new dataset.

For the original datasets presence of target habitat was determined from both quantitative and qualitative analysis of stills image data taken at 1 minute intervals along transects as described in Howell et al. (2010). *P. carpenteri* presence was determined from species lists from analysed sample data. *D. pertusum* reef habitat description follows that provided in Howell (2010), and subsequently adopted for use in the UK Deep Sea Habitat Classification (Parry et al. 2015). For the new independent dataset presence of the target habitat / species was determined by expert evaluation of image-based data alone. Habitat identification was undertaken by two annotators and designated when the habitat extent satisfied the OSPAR minimum biotope area threshold (25 m^2). For quality assurance, 5% of transects were independently analysed by Howell following inter-observer agreement standards used in published evidence (MacLeod et al., 2010).

2.3. Original Model Validation

For each of the four published models, the new biological dataset was plotted in ArcGIS on raster grids of published model output, in their respective output projections, and ROV point-based position data were reduced to one point per cell to avoid over-/under-weighting the importance of specific environmental conditions. Where cells contained any ROV position points interpreted as presence points, the one point per cell was denoted as a presence, all other points were denoted as absence. As the original models were masked for novel climates, new data points that did not sit on old model predictions were removed from the dataset as they were considered out of the original model domain. The final independent validation datasets for the 200 x 200m model included 2018 data points for *D. pertusum* reef and 1937 data points for *P. carpenteri* aggregations; for the 750 x 750 m model, the independent validation datasets included 646 data points for *D. pertusum* reef and 597 data points for *P. carpenteri* aggregations (Table 1). To assess the potential effect of spatial autocorrelation in inflating model performance, independent validation was also undertaken by reducing the datasets to one point per ROV transect. For each response variable a single presence point was randomly selected within each transect, and a single absence point from absence transects. This provided 173 and 163 validation points for the *D. pertusum* and *P. carpenteri* 200x200m models respectively and 186 and 182 validation points for the *D. pertusum* and *P. carpenteri* 750x750 models respectively.

The probability values from published model layers (coglog Maxent output) were extracted for each data point. Threshold independent metrics of model performance (Area Under the Receiver Operator Curve, AUC) for each model were calculated and compared to the original published models. Threshold dependent metrics of model performance (specificity,

sensitivity, and percent correctly classified) were also calculated by converting extracted probability values to binary presence-absence using 1) the thresholds defined in the original publications, and 2) new thresholds that maximised model performance against the new dataset.

2.4. Construction of new models

Newly collected high-resolution multibeam bathymetry data (Supplementary Material 1.0) were added to that described in Ross et al. (2015) and used to create grids of cell size 200x200 m that were re-projected from their original projection (WGS84) into Goode Homolosine Ocean (GHO) equal-area projection in order to allow for correct calculation of derived topographic layers and area.

2.4.1 Variable selection

Seven topographic variables were derived from the bathymetric data using the ArcGIS Benthic Terrain Modeller add-in (Walbridge et al. 2018): terrain ruggedness, curvature, plan curvature, profile curvature, slope, broad-scale bathymetric positions index (BBPI) and fine-scale bathymetric position index (FBPI). Information on the calculation and use of each of these variables can be found in the existing literature (Guinan et al. 2009, Ross & Howell 2013). The inner and outer radii for BBPI were 5 and 50 raster cells, respectively, facilitating identification of topographic features at 10 km scale such as canyons and hills. For FBPI, the inner and outer radiuses were 1 and 5 raster cells, respectively, allowing for the identification of features within the <1 km scale such as gullies. Generalised Additive Models (GAMs) were

248 used to build bottom temperature and salinity layers using *in-situ* CTD data from ROV and
249 drop camera transects, as well as archived CTD casts from the British Oceanographic Data
250 Centre (BODC) database. GAMs were implemented in R (R Core Team 2020) using the 'mcgv'
251 package (Wood 2011) with depth, latitude and longitude used as explanatory variables. A
252 detailed description is given in Supplementary Material 2.0. New and original biological
253 datasets for each of *D. pertusum* reef and *P. carpenteri* presence / absence were combined,
254 reprojected into GHO and plotted in ArcGIS on raster grids of environmental data. ROV/drop
255 camera point-based position data were reduced to one point per cell, where cells containing
256 any presence observations were denoted as a presence, all other points were denoted as
257 absence. Environmental data were extracted for each data point.

258 Maximum Entropy (MaxEnt) modelling (Phillips et al. 2006, Elith et al. 2011) is a presence-
259 background modelling technique that has a successful performance record (Elith et al. 2006),
260 particularly in studies with low prevalence (low number of presence records). Although
261 MaxEnt was designed to account for covariation in datasets and can perform well with
262 correlated variables (Feng et al., 2019), previous studies have found that pre-selection of
263 variables leads to better-performing models (Ross and Howell, 2013). Environmental
264 variables were therefore first assessed for covariance using correlation matrices and Variance
265 Inflation Factors in R. Strong correlations and VIFs between variables (≥ ±0.7 and ≥ 3,
266 respectively) were addressed by removing one variable from each correlated pair based on
267 the jackknife procedure. Jackknifing calculates the individual contribution of variables to a
268 model and produces model performance statistics (termed 'gain' in MaxEnt) for each. Once
269 correlates were removed, a model with all remaining variables was built. Following principles
270 of model parsimony, final sets of variables were selected by systematically removing the
271 variable contributing the least to the model (based on model gain with and without that

variable) until the drop in overall performance was deemed unacceptable. This process is described in detail in Supplementary Material 3.0 and 4.0.

2.4.2 Modelling

If used with presence-only data, MaxEnt randomly selects a specified number of 'background' points that are considered to represent locations with an equal likelihood of having been sampled that act as the absence points to inform the model (Elith et al. 2011). Whilst 'absence' points are presented in this study for each target taxa/habitat, it is not possible to be certain that they are not present somewhere within a 200 m grid cell due to the limited field-of-view of camera equipment compared to the size of grid cells, and therefore the data within this study represent 'pseudo-absences'. Having pseudo-absence data allowed for the MaxEnt samples-with-data (SWD) approach to be used whereby environmental values are provided in a spreadsheet for both the presence and pseudo-absence points, instead of allowing MaxEnt to randomly select background points to act as absences. The benefit of the SWD approach is that as both the presence and pseudo-absence points come from the same sampling campaigns, it allows for the control of some bias in sampling locations and experimental design that can facilitate improved predictive performance (Phillips & Dudík 2008).

Preliminary models with different parameters were systematically trialed, including the changing of feature classes (linear, quadratic, product, hinge and threshold) and the regularisation parameter (0.1, 0.5, 1, 3, 5, 10) to avoid over-fitting/-smoothing (Phillips & Dudík 2008). The final feature classes selected for both target habitat models were linear, quadratic and product features. Through trialing, hinge and threshold features were removed

295 due to lack of ecological applicability in this study; with these features turned on, the response
296 curves produced did not make biological sense. The *D. pertusum reef* model used a
297 regularisation parameter of 1, whilst the *P. carpenteri* model used 0.5. These parameters
298 were chosen because they struck a balance between the model overfitting and over-
299 generalising - this was apparent from the shape of the response curves and AUC scores. The
300 final MaxEnt models were projected onto the study area in a raster format and constrained
301 to sampled conditions using the MaxEnt novel climates output (i.e. areas where
302 environmental values fall within those on which the model was trained). Environmental data
303 layers used in the final models are plotted in Supplementary Material 5 and final model details
304 are provided in Supplementary Material 6.

305

306 2.5. Evaluation of New Models

307 Both presence and pseudo-absence records were used to evaluate the MaxEnt models'
308 performance by partitioning the data using a 70/30 split 10 times to create 10 sets of training
309 and test data. These datasets were compiled manually rather than using the automated
310 MaxEnt splitting tool to reduce spatial autocorrelation in the data. To achieve this, datasets
311 were split such that whole transects fell into either a training or testing dataset. This avoided
312 a scenario where a single transect would be split into training and testing points, leading to a
313 within-transect testing point validating the same transect (Howell et al. 2011). The prevalence
314 within each test and training dataset was compared to the prevalence of the full dataset and
315 any datasets identified as having >+/-1% change in the amount of presence data were
316 discarded and another random partition made until all test and train datasets satisfied the
317 criteria. Using the partitioned data, 10 new models were built for each habitat and evaluated

using the 'PresenceAbsence' package (Freeman & Moisen 2008) in R, employing both threshold-independent (AUC) and threshold-dependent metrics.

Three thresholding techniques were used to assess model performance, as suggested in Liu et al. (2009), and recognising that different thresholding methods seek to achieve different ends. Chosen thresholds were sensitivity-specificity equality (Sens=Spec), sensitivity-specificity sum maximisation (MaxSens+Spec) and minimum distance to the top left corner in the receiver operating characteristic curve plot (MinROCdist). Using the presence.absence.accuracy() function, the thresholding techniques and resulting model performances were assessed using three widely used indices: sensitivity, specificity and percent correctly classified (PCC). True skill statistic (TSS) can be calculated from sensitivity and specificity and is used in place of Cohen's kappa as it corrects the overall accuracy of the model predictions using the accuracy expected to occur by chance (Allouche et al., 2006). For both AUC and threshold-dependent metrics the mean and standard deviation for each metric was calculated for the 10 partitioned datasets and for the full model.

2.6. Quantification of Habitat Distribution and Marine Protected Area Analysis

The thresholding technique that gave the highest average of performance across the three chosen indices was selected for use in the final models. A binary raster of predicted presence and absence was produced as well as a raster of probability of predicted presence. Model fit was visualized by plotting the match-missmatch of binary predictions (Supplementary Material 7) In addition, the relative probability maps from all ten partitioned test/training models were used to produce standard deviation rasters to convey spatial uncertainty in the model predictions (Supplementary Material 8). The number of predicted presence raster cells

within different MPA polygons and below 800 m were calculated and then expressed as percentages of total presences in the whole study area, UK waters, and Irish waters. Values derived from published and new models were compared.

3. RESULTS

3.1. Original Model Validation

Results of the independent validation suggest that all published models perform worse than expected based on cross-validation results for both threshold dependent and independent metrics (Table 2 and 3). Model performance is still considered good (0.8–0.9) or fair (0.7–0.8) for scleractinian cold-water coral reef habitat models, with poorer performance for the *Pheronema carpenteri* models, particularly at low resolution. Independent validation using the thinned dataset of one point per ROV transect (removing effects of spatial autocorrelation) gave similar results. The extremely low prevalence of the *P. carpenteri* dataset (Table 1) mean that model performance as measured by PCC is very much influenced by correct prediction of absences (specificity), this also means threshold selection will be strongly influenced by specificity and might explain why the new thresholds are all very low . High-resolution models out-performed low-resolution models for both taxa.

3.2. New Models

Results of variable correlation analysis and step-by-step documentation of the variable pre-selection procedure are provided in Supplementary Material 3.0 and 4.0.

363 3.3. New Model Evaluation

364 Consideration of common performance indices (Table 4) allowed for selection of final
365 thresholding methods. For both models, Sens=Spec was selected as the chosen thresholding
366 method, providing thresholds for *D. pertusum* reef and *P. carpenteri* aggregations of 0.44 and
367 0.37, respectively. For *D. pertusum reef*, the AUC value for the full internally validated model
368 and all cross validation models was deemed excellent (0.9+).The 0.44 threshold determined
369 by Sens=Spec generated good (0.8+)results for PCC, sensitivity and specificity for all models.

370 For *P. carpenteri*, the AUC value for the full and all cross validation models was deemed
371 excellent. When thresholded at 0.26, all threshold-dependent metrics (PCC, sensitivity and
372 specificity) for the full and training *P. carpenteri* models were classified as excellent (0.9+ full
373 model and training sensitivity) or good (0.8-0.9 for training PCC and specificity) when
374 internally validated. All cross-validation models were classified as good (0.8-0.9).

375

376 3.4. New Model Variable Importance

377 When variables are considered in isolation for *D. pertusum reef*, model gain is highest for
378 temperature (70.5% contribution), followed by rugosity (23.3%) and FBPI (6.2%) as depicted
379 in the jackknife plot (Supplementary Material 6.0). Temperature also decreased the model
380 gain the most when removed as a variable, further illustrating its importance as the major
381 variable on which predictions are reliant. For the *P. carpenteri model*, when variables are
382 considered in isolation, model gain is highest for depth (41%) followed closely by temperature
383 (35.9%), then BBPI (20.1%) and profile curvature (3%). When omitted from the complete

384 model the variable that decreased model gain the greatest was depth, closely followed by
385 temperature.

386 3.5. Old (data poor) vs. New (data rich) high resolution models

387 Model performance determined by cross-validation suggests new models (Table 4) are
388 comparable but of lower performance than old models (Table 3). New model spatial
389 predictions in general follow those of the Ross et al. (2015) models, however, there are some
390 notable differences (Fig. 2). Cold-water coral reef is predicted present on all banks, seamounts
391 and the continental slope in the region, but the distribution is more restricted than that
392 predicted by Ross et al. (2015). As with the previous model, *P. carpenteri* is predicted present
393 on the continental slope, Porcupine Seabight, Rosemary Bank Seamount, around the Hatton-
394 Rockall Plateau, and particularly in the Hatton-Rockall Basin. Presence is also predicted near
395 the Wyville-Thomson Ridge where historical records refer to "the *Holtenia* grounds" (Wyville
396 Thomson, 1874). The most noticeable difference is in the change in predicted distribution in
397 the south-west section of the Hatton-Rockall Basin (circled in Fig. 2 c & d). Presence is
398 predicted for both taxa inside the existing MPA network but, following the overall trend, the
399 predicted distribution for *D. pertusum* reef is a contracted version of the 2015 predictions
400 (Fig. 3 a and b). Predictions for *P. carpenteri* presence inside MPAs has changed little from the
401 2015 model.

402

403 3.6. Comparison of percentage area protected by 2015 MPA network

404 For both taxa there is a significant reduction in predicted extent of suitable habitat in km^2 in
405 the new models when compared to the Ross & Howell (2013) and Ross et al. (2015) models

406 (Table 5). The difference is most striking for *D. pertusum* reef where the low-resolution 2013
407 model predicts an extent 39 times larger, and the 2015 model 6 times larger, than the new
408 model for the whole study area. Some of this reduction will be due to the removal of all *S.*
409 *variabilis* data points from the model data, which will have led to a slight contraction in
410 predicted depth range, however it is clear from Fig. 3 that there is a general contraction in
411 predicted distribution between new and old models. As *D. pertusum reefs* are only found
412 shallower than 1200m in this region, consideration of only those areas shallow than this depth
413 reveal the same over-all trend. However, there is an increase in the estimates of the
414 percentage of suitable habitat contained within the 2015 MPA network when calculated from
415 the new model as compared to old models.

416

417 3.7. Assessment of percentage area protected by the MPA network present in 2020

418 Assessment of the proportion of suitable habitat included within the present day MPA
419 network (Table 6) found that *D. pertusum* reef suitable environments are the most well
420 protected within the study area (~40% contained within MPAs) with protection at national
421 levels varying from 84% in UK to 24% in Irish waters. This is a significant increase from the 12-
422 32% protection under the 2015 network assessed using all models (Table 5). *P. carpenteri*
423 suitable habitat is the least well-protected of the two habitats assessed, with ~11% of
424 predicted suitable environments included within a current MPA, with protection at national
425 levels varying from ~49% in UK to ~4% in Irish waters. However, this again is a significant
426 increase on the 2015 MPA network, where the new model suggests only 7% of suitable
427 habitat was protected by the 2015 MPA network. The addition of new MPAs in UK waters
428 between 2015 and 2020 have taken the UK from around 59% to 84% protection for *D.*

pertusum reef and from 25% to 49% protection for *P. carpenteri*. It should be noted however that the Ross et al. (2015) and new model only cover a partial extent of the UK's continental shelf limit and data are biased to those areas that have been designated as MPAs. Thus, estimates of percentage protection are likely substantial overestimates. The EU ban on bottom trawling below 800m is estimated to protect 100% of the habitat suitable for *P. carpenteri*, and 42% of *D. pertusum* reef suitable habitat. Measured against IUCN targets both habitats are within or above the 20-30% protection level recommended.

4. DISCUSSION

4.1. Original Model Validation

Habitat suitability modelling (HSM) is a potentially valuable tool in the field of marine environmental management, but there remain questions around the true accuracy and reliability of modelled maps that may serve as a barrier to growth in use. In this study we have tested the performance of four published models at two different resolutions, 750x750 m (Ross & Howell 2013) and 200x200 m (Ross et al. 2015). Two for scleractinian cold water coral reef habitat and two for the sponge species *Pheronema carpenteri*. In the original published papers, all models performed well when tested using cross-validation methods, and performance was mixed when comparing low and high resolution models, according to threshold-dependent evaluation. While high-resolution *D. pertusum* reef models out performed low-resolution models, low-resolution models for *P. carpenteri* performed as well as high-resolution models according to threshold-dependent evaluation, and better than high resolution models according to threshold-independent evaluation (AUC). Our study has shown that when tested using independent data all models perform worse than

452 expected based on published cross-validation results for both threshold-dependent and
453 independent metrics. Although models perform worse than under cross-validation, model
454 performance is still considered good (0.9–0.8) or fair (0.8–0.7) for scleractinian cold-water
455 coral reef habitat models, with poorer performance for the *P. carpenteri* sponge models,
456 particularly at low resolution and when measured by sensitivity. High-resolution models
457 out-performed low-resolution models for both taxa when assessed using independent
458 data.

459 Our findings are in broad agreement with the very small number of comparable studies that
460 have independently validated deep-sea sponge and coral HSM published models, with some
461 notable differences. Rooper et al. (2016, 2018) independently validated HSM for corals and
462 sponges in the eastern Bering Sea slope, outer shelf in Alaska and Aleutian Islands. These
463 models were developed based on data from bottom trawl surveys at a resolution of
464 100x100 m grid cell size and validated using camera-based surveys. These studies found that
465 while model performance decreased when comparing cross-validation to independent AUC
466 scores, performance was still acceptable for coral models. This taken with our own findings
467 suggest that high resolution models (<200x200 m grid cell size) of deep-sea coral
468 distributions can be accurate and can provide useful information for spatial management of
469 these vulnerable taxa.

470 However, low-resolution models may not perform well. Bowden et al. (2021) recently
471 evaluated 47 HSM from eight published studies, all focused on the area around New
472 Zealand, using independent data. All models were at 1km or 30 arc-seconds grid cell size,
473 and in all cases model performance was lower than in published cross-validation values.
474 Anderson et al. (2016) found that their models of the distribution of four scleratinian species

475 (not *Desmophyllum pertusum*) across the South Pacific Regional Fisheries Management
476 Organisation area and adjoining EEZs were not successful in accurately predicting suitable
477 habitat for reef-forming deep-sea corals when independently validated. These models were
478 also constructed on a 30 arc-second grid (~1 km^2) and data resolution was given as a
479 possible explanation for model failure in the face of independent testing. Specifically, these
480 authors cited the limitations of the bathymetry dataset used, which in turn affected the
481 precision of each of the environmental predictor variables. Both studies report on models of
482 comparable resolution to the low-resolution Ross & Howell (2013) model tested here.

483 Interestingly the Ross & Howell (2013) model appears to have performed better than the
484 Anderson et al. (2016) models in the face of independent data. Anderson et al. (2016) cite
485 missing critical predictor variables, particularly substrate type, lack of true absence data,
486 spatial bias in distribution of presence records, and aspects of the topography in the study
487 area, as possible reasons for their model's poor performance. Ross & Howell's (2013) model
488 did make use of background data to account for spatial bias in the dataset, which may have
489 resulted in better performance when subjected to independent testing. However, a
490 principal difference between the Anderson et al. (2016) models and the Ross & Howell
491 (2013) model is the focus of the models. Ross & Howell (2013) modelled scleractinian reef
492 habitat where Anderson et al. (2016) modelled scleractinian species presence. The
493 difference is important as the former occupies a restricted subset of the environmental
494 niche of the latter (Howell et al. 2011), and a narrower niche width can result in a better
495 performing model (Kadmon et al. 2003, Tsoar et al. 2007). This concept is used to explain
496 the possible poor performance of Rooper et al.'s (2016, 2018) sponge models. These
497 authors suggested that the difference they observed in their high-resolution (100x100 m
498 grid cell size) coral and sponge model performance may be a result of lumping species

499 together into a large taxonomic group called ‘sponge’. This essentially merged species with
500 very different habitat preferences, ultimately giving the group a wide environmental niche.
501 The coral group in their study was dominated by a single family (Primnoidae) and thus was
502 less affected by this pooling action.

503 Niche width is unlikely to explain the poor performance of the *P. carpenteri* model. This
504 hexactinellid (glass sponge) is found predominantly on fine sediments where it loosely
505 anchors to the substrate using long spicules at the base of the organism. Aggregations in the
506 NE Atlantic are found over a very narrow depth range from 1000 to 1300 m (Rice et al.
507 1990) and appear to occupy a very specific niche. Cross-validation of HSMs created for this
508 species suggested model performance was excellent (Ross & Howell 2013, Ross et al. 2015).
509 However, independent validation suggests that while the models have fair to good PCC and
510 specificity, they have poor sensitivity, meaning that the resulting maps may be indicating an
511 absence where there is in fact a presence. Examination of the spatial distribution of false
512 negatives suggests most (25 of 28 data points) are found on offshore seamounts and banks.
513 These habitat types, and therefore this particular aspect of *P. carpenteri*’s environmental
514 niche, was not represented in the dataset used to build the published models and could
515 help explain why the models partially fail. However, aspects of the ecology of *P. carpenteri*
516 may also explain the poor model performance.

517 *P. carpenteri*, in common with other deep-sea sponge species that form aggregations, are
518 thought to be associated with regions of enhanced bottom currents related to the
519 interaction of internal waves with sloping boundaries (Rice et al. 1990, Klittgaard et al. 1997,
520 Davison et al. 2019) and raised features like the Mid-Atlantic Ridge (van Haren et al. 2017).
521 The causal link is suggested to be an increase in the supply of food as a result of the

resuspension of organic matter (Rice et al.1990). Oceanographic variables (and variability) may therefore be of critical importance in determining the distribution of *P. carpenteri*. The omission of such predictor variables from the Ross & Howell (2013) and Ross et al. (2015) models may also explain why both models partially fail when tested with independent data. The inclusion of oceanographic variables in deep-sea marine SDM has been found to improve model performance when tested with cross-validation (Rengstorf et al. 2014, Pearman et al. 2020) further supporting their inclusion in any future model development.

Our results suggest that for both scleractinian reef and *P. carpenteri*, the high-resolution models out-perform the low-resolution models when tested with independent data. This is an important finding as it suggests our ability to produce useful models of deep-sea benthic species and habitat distribution is dependent on availability of high-resolution environmental data including bathymetry data. Current maps of the seafloor are derived using satellite altimetry, which gives an average achievable resolution in the order of 8 km (Mayer et al. 2018). The percentage of the seafloor that has been measured by echo-sounders is considerably less than 18% and only about 9% of the seafloor is covered by high-resolution multibeam sonar data (Mayer et al. 2018). Recently an international effort has begun with the objective of facilitating the complete multibeam mapping of the world ocean by 2030. The Nippon Foundation GEBCO Seabed 2030 Project has the potential to improve significantly the quality of HSM it is possible to produce for deep-sea taxa by providing high-resolution bathymetry data. However, access to high-resolution oceanographic model output, as well as un-biased datasets of the distribution of target species and assemblages, and a good understanding of the biology and ecology of those species and assemblages, are also necessary to improve the quality of models. Targeted

efforts to collect these data over the next decade (Howell et al. 2020a,b) will be important in the further development of this field.

The good performance of the high-resolution scleractinian reef habitat model suggests that it may be a useful tool in the spatial management of cold-water coral reef in this region. Cold-water coral reef is considered a Vulnerable Marine Ecosystem (VME) under United Nations General Assembly Resolution 61/105, and, in the North East Atlantic is also classed as 'threatened and/or declining habitat' under the OSPAR Convention. Within European waters it is also recognised as an Annex I habitat under the EU Habitats and Species Directive (92/43/EEC). Collectively these policies require relevant management authorities to take actions to protect cold-water coral reef habitat. Specifically, UNGA 61/105 states "*In respect of areas where vulnerable marine ecosystems, including seamounts, hydrothermal vents and cold water corals, are known to occur or are likely to occur based on the best available scientific information, to close such areas to bottom fishing and ensure that such activities do not proceed unless conservation and management measures have been established to prevent significant adverse impacts on vulnerable marine ecosystems*". Actions have so far been limited to those areas where cold water coral reef has been observed either through visual or physical sampling means. However, the high-resolution model provides best available scientific information on where cold-water coral reef is likely to occur in this region, and thus could be used to support decisions around further measures.

Similarly, the good performance of the high-resolution *P. carpenteri* model in terms of PCC and specificity, and fair AUC score, suggests it also may be a useful tool in the spatial management of the region. However, it must be noted that this is a presence / absence

568 HSM, and therefore it only indicates likely presence / absence of suitable habitat for the
569 species (a VME indicator taxa), not the aggregation (a VME). This, together with the notable
570 deficiencies in the model outlined above, suggests it is less useful than the scleractinian reef
571 habitat model, but may still have value in indicating areas for further consideration given
572 the precautionary principle.

573

574 4.2. New Model performance and interpretation

575 The newly constructed high-resolution models for *D. pertusum reef* and *P. carpenteri* have
576 been developed using more than twice the input data used in the original Ross et al. (2015)
577 models (Table 1), and consideration of oceanographic predictor variables (temperature and
578 salinity) as terms in the models. Cross-validation suggests good performance for both models.
579 In general, model performance increases with increasing sample size, however the nature of
580 this relationship is variable and can depend on modelling method, prevalence, and species
581 range size (Stockwell & Peterson 2002, Wisz et al. 2008, van Proosdij et al. 2016). The inclusion
582 of oceanographic variables in deep-sea HSM has also been found to improve model
583 performance (Rengstorf et al. 2014, Pearman et al. 2020). This suggests that the new models
584 should perform better than the original 2015 models, although this can only be assessed using
585 new independent data.

586 In this study we have used a presence – background approach rather than a presence-absence
587 approach since our model input data are drawn from multiple surveys using multiple gear
588 types and spanning more than 30 years. In our opinion, absences cannot be inferred from our
589 dataset with certainty, and so we opted to be cautious in our use of absence data. However,
590 it should be noted that evidence suggests presence-absence models perform better than

591 presence-only models, particularly where species / assemblages occupy all suitable habitat,
592 making absence data reliable (Brotons et al. 2004), although Maxent has been found to
593 perform equally as well as presence-absence models (González-Irusta et al. 2014). Future
594 modelling efforts may wish to consider use of presence-absence approaches where authors
595 feel absence data are reliable.

596 Temperature was a significant term in both new models and is a fundamental variable that
597 controls species distributions. *D. pertusum* has been observed living under a wide range of
598 temperatures (4–13 °C) (Freiwald et al. 2004), with an upper thermal tolerance of 15 °C
599 (Brooke et al. 2013). Response curves for Maxent models for *D. pertusum reef*
600 (Supplementary Material 6.0) suggest the highest likelihood of occurrence of reef habitat in
601 the study area is at temperatures of ~8°C, which is almost the center of the species thermal
602 niche. There are no data available on the thermal niche of *P. carpenteri*. Howell et al. (2016)
603 reported this species to occur over a temperature range of 2.73–20.9 °C (mean 5.17 °C,
604 standard deviation 2.03) in the northern North Atlantic. Response curves for Maxent models
605 for *P. carpenteri* (Supplementary Material 6.0) suggest this species occupies a narrow thermal
606 niche, with peak likelihood of occurrence at between 6-8°C, falling sharply to no occurrences
607 below approximately 3°C or above 10°C. The wide range reported in Howell et al. (2016) is
608 likely a result of poor position data from the older records used in that model in order to
609 provide whole North Atlantic data coverage.

610 New model spatial predictions in general follow those of the Ross et al. (2015) models.
611 However, there are some notable differences, particularly in the spatial prediction for *P.*
612 *carpenteri* in the southern region of the Hatton-Rockall Basin (Fig. 2 c, d). In this region
613 available CTD data suggest the temperature is cooler than that at equivalent depths in the

614 Rockall Trough and on the European continental slope, making this region less suitable for *P.*
615 *carpenteri* than predicted by the 2015 model, which did not include temperature.
616 Interestingly the Howell et al. (2016) model, which did include temperature, also predicted
617 this area as suitable habitat, however the thermal niche of *P. carpenteri* was likely incorrectly
618 defined in that model as previously noted. The principal difference in the spatial predictions
619 for the *D. pertusum reef* model is a general contraction of the 2015 predictions in the current
620 model. This is well illustrated in Fig. 3 a and b where current model predictions are much
621 more focused than those of the 2015 model.

622

623 4.3. Re-assessment of current area closures and percentage protection targets for these VMEs

624 For both taxa there is a significant reduction in predicted extent in the new models when
625 compared to the Ross & Howell (2013) and Ross et al. (2015) models (Table 5). The 2013
626 low-resolution models predicted 39 times and 4 times greater extent for *D. pertusum reef*
627 and *P. carpenteri* respectively. This difference has important implications for onward use of
628 models in decision-making. For example, calculations of ecosystem services such as carbon
629 sequestration (Barnes et al. 2019; Barnes et al., 2021) or nutrient cycling (Hoffman et al.
630 2009) based on modelled extent may be grossly overestimated if based on low-resolution
631 models. Similarly, the 2015 models predicted a greater extent of suitable habitat than the
632 new model by 6 times and 1.4 times for *D. pertusum reef* and *P. carpenteri* respectively,
633 suggesting that estimates of extent based on model predictions should be used with
634 caution and considered likely overestimates.

635 In contrast, estimates of percentages of predicted suitable environments protected by the
636 regional MPA network increased when calculated using the new model compared to the

637 2013 and 2015 models. The Convention on Biological Diversity originally set out a target of
638 10% of marine areas to be protected by 2010 (UNEP/CBD/COP/DEC/VII/5) (later moved to
639 2020 (UNEP/CBD/COP/10/27)), and that is now being followed up with calls for 30% by 2030
640 (CBD, 2020). While these percentage area targets are not habitat specific, Aichi Target 11
641 makes specific reference to 'ecologically representative and well-connected systems of
642 protected areas' (UNEP/CBD/COP/10/27/Annex), which implies that different marine
643 habitat types should be protected at that level. The independently validated 2015 models
644 suggest that for the area modelled and the 2015 MPA network, both the UK and Ireland
645 have surpassed the original 10% protection target for *D. pertusum* reef, while the UK have
646 also surpassed this for *P. carpenteri* suitable habitat. In addition, the UK have surpassed the
647 30% target for *D. pertusum* reef habitat in the modelled area. The picture is the same for the
648 new model. However, in both the 2015 and new model, Ireland protects <10% of suitable
649 habitat for *P. carpenteri*, implying that further MPAs may be required. Ireland has
650 committed to protecting 30% of its habitat by 2030 (Marine Protected Area Advisory Group,
651 2020) and data such as these can help guide that process.

652 The situation is broadly similar when considering the 2020 MPA network although the
653 estimates of percentage of habitat protected in UK waters are much higher. It must,
654 however, be noted that the current MPA network is not 'strictly protected' in line with IUCN
655 specifications and in some cases management measures have yet to be drawn up. It is also
656 important to remember that the modelled area in UK waters is much more limited than that
657 modelled in Irish waters due to the limited availability of multibeam mapping in UK waters.
658 The areas that have been mapped (and thus modelled onto) in UK waters tend to be
659 associated with protected status, thus the UK figures are likely gross overestimates.
660 Estimates of percentage of suitable habitat made from the low resolution 2013 model are

lower than all other estimates, and, reiterating the findings of Ross et al. (2015), suggests that low-resolution models result in conservative estimates in this context, which is in line with the precautionary principle and suggests low-resolution models may have a use in this area.

An interesting finding is that the ban on bottom trawling below 800 m in EU waters (UK is currently following) protects >30% of both habitats estimated from the new model with 100% of *P. carpenteri* suitable habitat protected. While a significant achievement, it is important to again consider the issue of representativeness in Aichi Target 11. Cold-water coral reefs occurring at different depths support different assemblages of associated species in line with the well-documented turnover of species along the depth gradient (Rowe & Menzies 1969, Howell et al. 2002, Carney 2005). In order to be representative, protection for cold-water coral reef sites must span its known depth range (thermal niche) necessitating protection of sites shallower than 800 m. In addition, the twin threats of ocean acidification and global warming mean that shallower areas of predicted suitable habitat in this region may be key refuge sites for cold-water coral reef (Jackson et al. 2014). Ocean acidification is causing the aragonite saturation horizon (ASH) to shoal exposing deep-water coral reefs to waters that are corrosive to coral skeletons (Guinotte et al. 2006). In parallel, seawater temperatures are increasingly exposing reefs to novel conditions. While live *D. pertusum* can tolerate long-term exposure to combined end-of-the-century temperature and pCO_2 scenarios (Hennige et al. 2015, Büscher et al. 2017), the dead coral skeletons that make up the reef framework are weakened by acidified conditions and become more susceptible to bioerosion and mechanical damage (Hennige et al. 2015). This ultimately leads to crumbling, collapse, and loss of complexity of the larger habitat, and resulting ecosystem services (Hennige et al. 2020). In this region, the East Mingulay Special Area of Conservation (SAC), Wyville Thomson Ridge SAC,

and North West Rockall Bank SAC represent important strongholds for reef habitat (Jackson et al. 2014) and therefore the 800 m bottom-trawling ban alone will not meet the qualitative aims of Aichi Target 11.

5. CONCLUSION

Independent testing of four published models has shown that for the taxa considered, high-resolution models (<200x200 m grid cell size) can be accurate and can provide useful information for spatial management of these vulnerable taxa. With respect to UNGA Resolution 61/105, the high-resolution cold-water coral reef model provides best available scientific information on where this VME is likely to occur in this region, and thus could be used to support decisions around further measures. Our ability to produce useful models of deep-sea benthic species and habitat distribution is highly dependent on the availability of high-resolution environmental data including bathymetry data. To improve model performance significant research effort is needed to map the seafloor, oceanographic environment, and distribution of species and assemblages (presence, absences, density) in order to provide more, better quality, model input data. In addition, further research effort is needed to provide a more complete understanding of the importance of environmental variables to target taxa, and their interactions at a variety of scales. For well performing high-resolution models (200x200m), estimates of extent based on model predictions should be used with caution and considered likely overestimates. Low-resolution models (750x750m) may be useful in providing conservative estimates in progress towards percentage protection targets but are not recommended for use in estimates of extent. For *D. pertusum* reef and *P. carpenteri* the UK and Ireland have made good progress towards

708 the 10% CBD target for conserving habitats and species within MPAs. This together with the
709 EU ban on bottom trawling below 800 m, provide a level of protection for both, however
710 representativity needs to be considered in these assessments. Assessment of UK progress is
711 limited by a lack of available multibeam data.

712

713 **6. ACKNOWLEDGEMENTS**

714 We would like to thank the scientists, officers and crew of all research cruises that have
715 contributed to the collection of data for this study. The 2015 data collection on RV Celtic
716 Explorer was funded under the European Union's FP7 Research Infrastructures Programme
717 under the grant agreement 312762 (EUROFLEETS2). The 2016 data collection was funded by
718 the UK Natural Environment Research Council, grant number NE/K011855/1 - DeepLinks
719 project. SeaRover reef habitat data acquired offshore Ireland during 2017, 2018, and 2019
720 have kindly been made available by the Government of Ireland in support of this research.
721 The Sensitive Ecosystem Assessment and ROV Exploration of Reef (SeaRover) was
722 commissioned by the Marine Institute in partnership with National Parks and Wildlife
723 Service (NPWS), and funded by the European Maritime and Fisheries Fund (EMFF),
724 Department of Agriculture, Food and the Marine (DAFM) & NPWS. The project was
725 coordinated by the Department of Environment, Climate & Communications funded
726 INFOMAR programme team, with research support from National University Ireland Galway,
727 Plymouth University, and Institute of Marine Research Norway. INFOMAR is jointly managed
728 by Marine Institute & Geological Survey Ireland. This article is delivered under the MISSION
729 ATLANTIC project funded by the European Union's Horizon 2020 Research and Innovation
730 Program under grant agreement No. 639 862428. The following persons offered support in

data collection and advice throughout: David O'Sullivan, Yvonne Leahy, Janine Guinan, Nils Piechaud. This study uses CTD data provided by the British Oceanographic Data Centre.

7. REFERENCES

Addison PF, Rumpff L, Bau SS, Carey JM, Chee YE, Jarrad FC, McBride MF, Burgman MA, (2013) Practical solutions for making models indispensable in conservation decision-making. Divers Distrib 19:490-502

Allouche, O, Tsoar, A and Kadmon, R, (2006) Assessing the accuracy of species distribution models: prevalence, kappa and the true skill statistic (TSS). J Appl Ecol 43:1223-1232

Anderson OF, Guinotte JM, Rowden AA, Clark MR, Mormede S, Davies AJ, Bowden DA (2016) Field validation of habitat suitability models for vulnerable marine ecosystems in the South Pacific Ocean: implications for the use of broad-scale models in fisheries management. Ocean Coast Manag 120:110-126

Andréfouët S, Muller-Karger FE, Robinson JA, Kranenburg CJ, Torres-Pullizza D, Spraggins SA, Murch B (2006) Global assessment of modern coral reef extent and diversity for regional science and management applications: a view from space. In: Suzuki Y, Nakamori T, Hidaka M, Kayanne H and others (eds) Proceedings of 10th International Coral Reef Symposium. Japanese Coral Reef Society, Okinawa, p 1732−1745

Auster PJ (2005) Are deep-water corals important habitats for fishes? In: Freiwald A. Roberts JM (eds) Cold-Water Corals and Ecosystems. Springer-Verlag, Berlin, Heidelberg, p 747-760

Barnes DK, Sands CJ, Richardson A, Smith N (2019) Blue carbon natural capital shallower than 1000 m in isolated, small and young Ascension Island's EEZ. Front Mar Sci 6:663

753 Barnes DK, Bell JB, Bridges AE, Ireland L, Howell KL, Martin SM, Sands CJ, Mora Soto A, Souster
754 T, Flint G, Morley SA (2021) Climate mitigation through biological conservation: Extensive and
755 valuable blue carbon natural capital in Tristan da Cunha's giant Marine Protected Zone.
756 Biology, 10:1339

757 Bett BJ, Rice AL (1992) The influence of hexactinellid sponge (*Pheronema carpenteri*) spicules
758 on the patchy distribution of macrobenthos in the Porcupine Seabight (bathyal NE Atlantic).
759 Ophelia 36:217-226

760 Bowden DA, Anderson OF, Rowden AA, Stephenson F, Clark MR (2021) Assessing Habitat
761 Suitability Models for the Deep Sea: Is Our Ability to Predict the Distributions of Seafloor
762 Fauna Improving? Front Mar Sci 8:239

763 Brooke S, Ross SW, Bane JM, Seim HE, Young CM (2013) Temperature tolerance of the deep-
764 sea coral *Lophelia pertusa* from the south-eastern United States. Deep-Sea Res II 92:240-248

765 Brotons L, Thuiller W, Araújo MB, Hirzel AH (2004) Presence-absence versus presence-only
766 modelling methods for predicting bird habitat suitability. Ecography, 27:437-448

767 Bryan TL, Metaxas A (2007) Predicting suitable habitat for deep-water gorgonian corals on
768 the Atlantic and Pacific Continental Margins of North America. Mar Ecol Prog Ser 330:113-126

769 Büscher JV, Form AU, Riebesell U (2017) Interactive effects of ocean acidification and warming
770 on growth, fitness and survival of the cold-water coral *Lophelia pertusa* under different food
771 availabilities. Front Mar Sci 4:101

772 Carney RS (2005) Zonation of deep-sea biota on continental margins. Oceanogr Mar Biol Annu
773 Rev 43:211–279

774 Davison JJ, van Haren H, Hosegood P, Piechaud N, Howell KL (2019) The distribution of deep-
775 sea sponge aggregations (Porifera) in relation to oceanographic processes in the Faroe-
776 Shetland Channel. Deep-Sea Res Pt I 146:55-61.

777 Elith JH, Graham CP, Anderson R, Dudík M, Ferrier S, Guisan AJ, Hijmans R, Huettmann FR,
778 Leathwick J, Lehmann A, Li J (2006) Novel methods improve prediction of species'
779 distributions from occurrence data. Ecography 29:129-151.

780 Elith J, Phillips SJ, Hastie T, Dudík M, Chee YE, Yates CJ (2011) A statistical explanation of
781 MaxEnt for ecologists. Divers Distrib 17:43-57.

782 Feng X, Park DS, Liang Y, Pandey R, Papeş M (2019) Collinearity in ecological niche modeling:
783 Confusions and challenges. Ecol Evol 9:10365-10376.

784 Foubert A, Beck T, Wheeler AJ, Opderbecke J, Grehan A, Klages M, Thiede J, Henriet JP
785 Polarstern AX (2005). New view of the Belgica Mounds, Porcupine Seabight, NE Atlantic:
786 preliminary results from the Polarstern ARK-XIX/3a ROV cruise. In: Freiwald A, Roberts JM,
787 (eds) Cold-Water Corals and Ecosystems. Springer-Verlag, Berlin, Heidelberg, p 403-415

788 Freiwald A, Fosså JH, Grehan A, Koslow T, Roberts JM (2004) Coldwater Coral Reefs. UNEP-
789 WCMC, Cambridge

790 González-Irusta JM, González-Porto M, Sarralde R, Arrese B, Almón B, Martín-Sosa P (2015)
791 Comparing species distribution models: a case study of four deep sea urchin
792 species. Hydrobiologia, 745:43-57

793 Guinan J, Brown C, Dolan MF, Grehan AJ (2009) Ecological niche modelling of the distribution
794 of cold-water coral habitat using underwater remote sensing data. Ecol Inform 4:83-92

795 Guinotte JM, Orr J, Cairns S, Freiwald A, Morgan L, George R (2006) Will human-induced
796 changes in seawater chemistry alter the distribution of deep-sea scleractinian corals? Front
797 Ecol Environ 4:141-146

798 Hansen MC, Potapov PV, Moore R, Hancher M, Turubanova SAA, Tyukavina A, Thau D,
799 Stehman SV, Goetz SJ, Loveland TR, Kommareddy A, Egorov A, Chini L, Justice CO, Townshend
800 JRG (2003) High-Resolution Global Maps of 21st-Century Forest Cover Change. Science
801 342:850–853

802 Hennige SJ, Wicks LC, Kamenos NA, Perna G, Findlay HS, Roberts JM (2015) Hidden impacts
803 of ocean acidification to live and dead coral framework. Proc Roy Soc B 282: 20150990.

804 Hennige SJ, Wolfram U, Wickes L, Murray F, Roberts JM, Kamenos NA, Schofield S, Groetsch
805 A, Spiesz EM, Aubin-Tam ME, Etnoyer PJ (2020) Crumbling Reefs and Cold-Water Coral Habitat
806 Loss in a Future Ocean: Evidence of “Coralporosis” as an Indicator of Habitat Integrity. Front
807 Mar Sci 7:668

808 Hilborn, R., 2012. The evolution of quantitative marine fisheries management 1985–2010. Nat
809 Resour Model 25:122-144.

810 Hijmans RJ (2012) Cross-validation of species distribution models: removing spatial sorting
811 bias and calibration with a null model. Ecol 93:679-688

812 Hoffmann F, Radax R, Woebken D, Holtappels M, Lavik G, Rapp HT, Schläppy ML, Schleper C,
813 Kuypers MM (2009) Complex nitrogen cycling in the sponge *Geodia barretti*. Environ
814 Microbiol 11:2228-2243

Howell KL, Billett DSM, Tyler PA (2002) Depth-related distribution and abundance of seastars (Echinodermata: Asteroidea) in the Porcupine Seabight and Porcupine Abyssal Plain, N.E. Atlantic. Deep-Sea Res I 49:1901–1920

Howell KL (2010) A benthic classification system to aid in the implementation of marine protected area networks in the deep/high seas of the NE Atlantic. Biol Conserv 143:1041-1056

Howell KL, Davies JS, Narayanaswamy BE (2010) Identifying deep-sea megafaunal epibenthic assemblages for use in habitat mapping and marine protected area network design. J Mar Biol Assoc UK 90:33

Howell KL, Holt R, Endrino IP, Stewart H (2011) When the species is also a habitat: comparing the predictively modelled distributions of *Lophelia pertusa* and the reef habitat it forms. Biol Conserv 144:2656-2665

Howell KL, Huvenne V, Piechaud N, Robert K, Ross RE (2014) Analysis of Biological Data From the JC060 Survey of Areas of Conservation Interest in Deep Waters off North and West Scotland. JNCC Report No. 528. JNCC. Peterborough.

Howell KL, Piechaud N, Downie AL, Kenny A (2016) The distribution of deep-sea sponge aggregations in the North Atlantic and implications for their effective spatial management. Deep-Sea Res I 115:309-320

Howell KL, Hilário A, Allcock AL, Bailey D, Baker M, Clark MR, Colaço A, Copley J, Cordes EE, Danovaro R, Dissanayake A et al. (2020) A decade to study deep-sea life. Nat Ecol Evol 5:265-267

835 Howell KL, Hilário A, Allcock AL, Bailey D, Baker M, Clark MR, Colaço A, Copley J, Cordes EE,
836 Danovaro R, Dissanayake A et al. (2020) A blueprint for an inclusive, global deep-sea Ocean
837 Decade field program. Front Mar Sci 7:999.

838 Hughes DJ, Gage JD (2004) Benthic metazoan biomass, community structure and bioturbation
839 at three contrasting deep-water sites on the northwest European continental margin. Prog
840 Oceanogr 63:29-55

841 Husebø Å, Nøttestad L, Fosså JH, Furevik DM, Jørgensen SB (2002) Distribution and abundance
842 of fish in deep-sea coral habitats. Hydrobiol 471:91-99

843 Huvenne VA, Beyer A, de Haas H, Dekindt K, Henriet JP, Kozachenko M, Olu-Le Roy K, Wheeler
844 AJ (2005) The seabed appearance of different coral bank provinces in the Porcupine Seabight,
845 NE Atlantic: results from sidescan sonar and ROV seabed mapping. In: Freiwald A, Roberts JM,
846 (eds) Cold-Water Corals and Ecosystems. Springer-Verlag, Berlin, Heidelberg, p 535–569.

847 IPCC (2014) Climate Change 2014: Synthesis Report. Contribution of Working Groups I, II and
848 III to the Fifth Assessment Report of the Intergovernmental Panel on Climate Change [Core
849 Writing Team, R.K. Pachauri and L.A. Meyer (eds.)]. IPCC, Geneva, Switzerland, 151 pp.

850 Jackson EL, Davies AJ, Howell KL, Kershaw PJ, Hall-Spencer JM (2014) Future-proofing marine
851 protected area networks for cold-water coral reefs. ICES J Mar Sci 71:2621-2629.

852 Kadmon R, Farber O, Danin A (2003) A systematic analysis of factors affecting the
853 performance of climatic envelope models. Ecol Appl 13:853-867

854 Kenyon NH, Ivanov MK, Akhmetzhanov AM (1998) Cold-water carbonate mounds and
855 sediment transport on the Northeast Atlantic Margin. IOC Technical Series. UNESCO, Paris.

856 Kim YJ, Gu C (2004) Smoothing spline Gaussian Regression: More scalable computation via
857 efficient approximation. J Roy Stat Soc B 66:337-356

858 Klitgaard AB, Tendal OS, Westerberg H (1997) Mass occurrences of large sponges (Porifera) in
859 Faroe Island (NE Atlantic) shelf and slope areas: characteristics, distribution and possible
860 causes. In: Jensen AC, Shbeader M, Williams JA (eds) Responses of marine organisms to their
861 environments. Proc 30th Eur Mar Biol Symp. University of Southampton, Southampton. p
862 129–142.

863 Lavaleye MSS, Duineveld GCA, Berghuis EM, Kok A, Witbaard R (2002) A comparison between
864 the megafauna communities on the NW Iberian and Celtic continental margins—effects of
865 coastal upwelling? Prog Oceanogr 52:459-476.

866 Le Danois E (1948) Les profondeurs de la mer: trente ans de recherches sur la faune sous-
867 marine au large des cotes de France, Payot, Paris.

868 Marine Protected Area Advisory Group (2020). Expanding Ireland's Marine Protected Area
869 Network: A report by the Marine Protected Area Advisory Group. Report for the Department
870 of Housing, Local Government and Heritage, Ireland.

871 Marshall CE, Glegg GA, Howell KL (2014) Species distribution modelling to support marine
872 conservation planning: the next steps. Mar Policy 45:330-332

873 Mayer L, Jakobsson M, Allen G, Dorschel B, Falconer R, Ferrini V, Lamarche G, Snaith H,
874 Weatherall P (2018) The Nippon Foundation—GEBCO seabed 2030 project: The quest to see
875 the world's oceans completely mapped by 2030. Geosci, 8:63.

876 MacLeod, N., Benfield, M. and Culverhouse, P., 2010. Time to automate identification. Nature,
877 467(7312), pp.154-155.

878 Mienis F, van Weering T, de Haas H, de Stigter H, Huvenne V, Wheeler A (2006) Carbonate
879 mound development at the SW Rockall Trough margin based on high resolution TOBI and
880 seismic recording. Mar Geol 233:1–19

881 Pearman TRR, Robert K, Callaway A, Hall R, Iacono CL, Huvenne VA (2020) Improving the
882 predictive capability of benthic species distribution models by incorporating oceanographic
883 data–Towards holistic ecological modelling of a submarine canyon. Prog Oceanogr 184,
884 p.102338

885 Piechaud, N., Downie, A., Stewart, H.A. and Howell, K.L., 2014. The impact of modelling
886 method selection on predicted extent and distribution of deep-sea benthic assemblages.
887 Earth Environ Sci Trans R Soc Edinb 105:251-261

888 R Core Team (2020) R: A language and environment for statistical computing. R Foundation
889 for Statistical Computing, Vienna.

890 Rees SE, Foster NL, Langmead O, Pittman S, Johnson DE (2018) Defining the qualitative
891 elements of Aichi Biodiversity Target 11 with regard to the marine and coastal environment
892 in order to strengthen global efforts for marine biodiversity conservation outlined in the
893 United Nations Sustainable Development Goal 14. Mar Policy 93:241-250

894 Reiss H, Birchenough S, Borja A, Buhl-Mortensen L, Craeymeersch J, Dannheim J, Darr A,
895 Galparsoro I, Gogina M, Neumann H, Populus J (2015) Benthos distribution modelling and its
896 relevance for marine ecosystem management. ICES J Mar Sci 72:297-315

897 Rengstorf AM, Mohn C, Brown C, Wisz MS, Grehan AJ (2014) Predicting the distribution of
898 deep-sea vulnerable marine ecosystems using high-resolution data: Considerations and novel
899 approaches. Deep-Sea Res I 93:72-82

900 Rice AL, Thurston MH, New AL (1990) Dense aggregations of a hexactinellid sponge,
901 *Pheronema carpenteri*, in the Porcupine Seabight (northeast Atlantic Ocean), and possible
902 causes. Prog Oceanogr 24:179-196.

903 Robert K, Jones DO, Roberts JM, Huvenne VA (2016) Improving predictive mapping of deep-
904 water habitats: Considering multiple model outputs and ensemble techniques. Deep-Sea Res
905 I 113:80-89

906 Roberts JM, Brown CJ, Long D, Bates CR (2005) Acoustic mapping using a multibeam
907 echosounder reveals cold-water coral reefs and surrounding habitats. Coral Reefs, 24:654-
908 669

909 Roberts JM, Wheeler AJ, Freiwald A (2006) Reefs of the deep: the biology and geology of cold-
910 water coral ecosystems. Science 312:543-547

911 Rooper CN, Sigler MF, Goddard P, Malecha P, Towler R, Williams K, Wilborn R, Zimmermann
912 M (2016) Validation and improvement of species distribution models for structure-forming
913 invertebrates in the eastern Bering Sea with an independent survey. Mar Ecol Prog Ser
914 551:117-130

915 Rooper CN, Wilborn R, Goddard P, Williams K, Towler R, Hoff GR (2018). Validation of deep-
916 sea coral and sponge distribution models in the Aleutian Islands, Alaska. ICES J Mar Sci 75:199-
917 209.

918 Ross LK, Ross RE, Stewart HA, Howell KL (2015) The influence of data resolution on predicted
919 distribution and estimates of extent of current protection of three 'listed' deep-sea habitats.
920 PLoS One, 10:p.e0140061.

921 Ross RE, Howell KL (2013) Use of predictive habitat modelling to assess the distribution and
922 extent of the current protection of 'listed' deep-sea habitats. Divers Distrib 19:433-445

923 Ross RE, Wort EJ, Howell KL (2019) Combining distribution and dispersal models to identify a
924 particularly vulnerable marine ecosystem. Front Mar Sci 6:574

925 Rowden AA, Anderson OF, Georgian SE, Bowden DA, Clark MR, Pallentin A, Miller A (2017)
926 High-resolution habitat suitability models for the conservation and management of
927 vulnerable marine ecosystems on the Louisville Seamount Chain, South Pacific Ocean. Front
928 Mar Sci 4:335

929 Rowe GT, Menzies RJ (1969) Zonation of large benthic invertebrates in the deep-sea off the
930 Carolinas. Deep-Sea Res I 16:531–537

931 Sillero N, Barbosa AM (2021) Common mistakes in ecological niche models. Int J Geogr Inf
932 Sci 35:213-226

933 Stirling DA, Boulcott P, Scott BE, Wright PJ (2016) Using verified species distribution models
934 to inform the conservation of a rare marine species. Divers Distrib 22:808-822

935 Stockwell DR, Peterson AT (2002) Effects of sample size on accuracy of species distribution
936 models. Ecol Modell 148:1-13

937 Traganos D, Aggarwal B, Poursanidis D, Topouzelis K, Chrysoulakis N, Reinartz P (2018)
938 Towards global-scale seagrass mapping and monitoring using Sentinel-2 on Google Earth
939 Engine: The case study of the Aegean and Ionian seas. Remote Sens 10:1227

940 Tsoar A, Allouche O, Steinitz O, Rotem D, Kadmon R (2007) A comparative evaluation of
941 presence-only methods for modelling species distribution. Divers Distrib 13:397-405

942 UN General Assembly, Transforming Our World: The 2030 Agenda for Sustainable
943 Development. http://www.refworld.org/docid/57b6e3e44.html. Accessed: 1st August 2021

944 UNEP-WCMC, WorldFish Centre, WRI, TNC (2018) Global distribution of warm-water coral
945 reefs, compiled from multiple sources including the Millennium Coral Reef Mapping Project.
946 Version 4.0. UN Environment World Conservation Monitoring Centre, Cambridge.

947 van Proosdij AS, Sosef MS, Wieringa JJ, Raes N (2016) Minimum required number of specimen
948 records to develop accurate species distribution models. Ecography 39:542-552

949 Veloz SD (2009) Spatially autocorrelated sampling falsely inflates measures of accuracy for
950 presence-only niche models. J Biogeogr 36:2290-2299

951 Vieira RP, Bett BJ, Jones DO, Durden JM, Morris KJ, Cunha MR, Trueman CN, Ruhl HA (2020)
952 Deep-sea sponge aggregations (*Pheronema carpenteri*) in the Porcupine Seabight (NE
953 Atlantic) potentially degraded by demersal fishing. Prog Oceanogr 183: p102189

954 Webb TJ, Berghe EV, O'Dor R (2010) Biodiversity's big wet secret: the global distribution of
955 marine biological records reveals chronic under-exploration of the deep pelagic ocean. *PLoS*
956 *One 5:*(8) p.e10223

957 Wheeler AJ, Beyer A, Freiwald A, de Haas H, Huvenne VAI, Kozachenko M, Roy KOL,
958 Opderbecke J (2007) Morphology and environment of cold-water coral carbonate mounds on
959 the NW European margin. Int J Earth Sci 96:37-56

960 Wienberg C, Beuck L, Heidkamp S, Hebbeln D, Freiwald A, Pfannkuche O, Monteys X (2008)
961 Franken Mound: facies and biocoenoses on a newly-discovered “carbonate mound” on the
962 western Rockall Bank, NE Atlantic. Facies 54:1-24

963 Wisz MS, Hijmans RJ, Li J, Peterson AT, Graham CH, Guisan A, NCEAS Predicting Species
964 Distributions Working Group (2008) Effects of sample size on the performance of species
965 distribution models. Divers Distrib 14:763-773

966 Wood SN (2011) Fast stable restricted maximum likelihood and marginal likelihood estimation
967 of semiparametric generalized linear models. J Roy Stat Soc B 73:3-36

968 Wyville Thomson C (1874) *Depths of the Sea.* Macmillan and Co, London.

969

970 Table 1: Breakdown, total (presence/absence), of biological datasets used to build habitat
971 suitability models and independently validate Ross & Howell (2013) and Ross *et al.* (2015).

	Ross & Howell 2013 (GEBCO)	Ross *et al.* 2015 (200m)	Howell *et al.* 2021	Ross & Howell 2013 (GEBCO) Validation	Ross *et al.* 2015 (200m) Validation
D. pertusum	864 (75/789)	1,284 (116/1,168)	3,291 (227/3,064)	646 (64/582)	2,018 (122/1896)
P. carpenteri	864 (53/811)	1,284 (74/1,210)	3,196 (139/3,057)	597 (32/565)	1,937 (66/1871)

972

973 Table 2: Performance statistics for the published Ross & Howell (2013) models according to
974 original cross validation and new independent validation. Threshold values are predicted
975 probabilities of presence. SD = Standard deviation.

	Method	**PCC (SD)**	**Sens. (SD)**	**Spec. (SD)**	**TSS (Sens+ Spec-1)**	**AUC (SD)**	**Threshold values**
***D. pertusum* reef**							
Original cross validation with original threshold (Ross & Howell 2013)	MinROCdist	0.82	0.75	0.82	0.57	0.86	0.48
Independent validation with original threshold.		0.68 (0.02)	0.78 (0.05)	0.67 (0.02)	0.45	0.74 (0.02)	0.48
Independent validation but tuned to maximize model performance (new threshold selected)	Sens=Spec	0.70 (0.02)	0.70 (0.06)	0.70 (0.02)	0.40	0.74	0.50
Independent validation with original threshold and thinned dataset.	MinROCdist	0.77 (0.03)	0.71 (0.08)	0.78 (0.03)	0.49	0.79 (0.04)	0.48
Independent validation but tuned to maximize model performance (new threshold selected) using thinned dataset	Sens=Spec	0.73 (0.03)	0.74 (0.07)	0.73 (0.04)	0.47	0.79 (0.04)	0.44
P. carpenteri							
Original cross validation with original threshold (Ross & Howell 2013)	MinROCdist	0.95	0.96	0.95	0.91	0.99	0.19
Independent validation with original threshold.		0.91 (0.01)	0.34 (0.09)	0.95 (0.01)	0.29	0.65 (0.05)	0.19

Independent validation but tuned to maximize model performance (new threshold selected)	MaxSens+ Spec	0.92 (0.01)	0.34 (0.09)	0.95 (0.01)	0.30	0.66 (0.05)	0.45
Independent validation with original threshold and thinned dataset.	MinROCdist	0.89 (0.02)	0.31 (0.12)	0.95 (0.02)	0.26	0.71 (0.07)	0.19
Independent validation but tuned to maximize model performance (new threshold selected) using thinned dataset	MaxSens+ Spec	0.90 (0.02)	0.31 (0.12)	0.95 (0.02)	0.26	0.71 (0.07)	0.375

976

977 Table 3: Performance of the published Ross et al. (2015) models according to original cross
978 validation and new independent validation. Threshold values are predicted probabilities of
979 presence. SD = Standard deviation.

	Method	**PCC (SD)**	**Sens. (SD)**	**Spec. (SD)**	**TSS (Sens+ Spec-1)**	**AUC (SD)**	**Threshold values**
***D. pertusum* reef**							
Original cross validation with original threshold (Ross et al. 2015)	MinROCdist	0.85	0.85	0.85	0.70	0.91	0.43
Independent validation with original threshold.		0.72 (0.01)	0.88 (0.03)	0.70 (0.01)	0.58	0.87	0.43
Independent validation but tuned to maximize model performance (new threshold selected)	Sens=Spec	0.77 (0.01)	0.75 (0.04)	0.77 (0.01)	0.52	0.87 (0.01)	0.48
Independent validation with original threshold and thinned dataset.		0.82 (0.03)	0.82 (0.07)	0.82 (0.03)	0.64	0.90 (0.03)	0.43

Independent validation but tuned to maximize model performance (new threshold selected) using thinned dataset	Sens=Spec	0.82 (0.03)	0.82 (0.07))	0.82 (0.03)	0.64	0.90 (0.03)	0.435
P. carpenteri							
Original cross validation with original threshold (Ross et al. 2015)	MinROCdist	0.96	0.96	0.96	0.92	0.96	0.34
Independent validation with original threshold.		0.90 (0.01)	0.47 (0.06)	0.91 (0.01)	0.29	0.69 (0.04)	0.34
Independent validation but tuned to maximize model performance (new threshold selected)	MaxSens+ Spec	0.84 (0.01)	0.67 (0.06)	0.84 (0.01)	0.51	0.74 (0.04	0.07
Independent validation with original threshold and thinned dataset.		0.86 (0.03)	0.47 (0.13)	0.90 (0.02)	0.37	0.75 (0.08)	0.34
Independent validation but tuned to maximize model performance (new threshold selected) using thinned dataset	MaxSens+ Spec	0.84 (0.03)	0.6 (0.13)	0.86 (0.03)	0.46	0.75 (0.08)	0.175

Table 4: Threshold-dependent evaluation indices for training, test, and full models. Final thresholds and associated evaluation metrics shaded.

	Average Training – Internal validation			**Average Test – Cross validation**			**Full Model – Internal validation**			
Thresholding approach	**PCC (SD)**	**Sens. (SD)**	**Spec. (SD)**	**PCC (SD)**	**Sens. (SD)**	**Spec. (SD)**	**PCC (SD)**	**Sens. (SD)**	**Spec. (SD)**	**Threshold**
***D. pertusum* reef**										
Sens=Spec	0.83 (0.01)	0.82 (0.03)	0.83 (0.01)	0.83 (0.01)	0.83 (0.05)	0.83 (0.01)	0.83 (0.01)	0.82 (0.03)	0.83 (0.01)	0.44
MaxSens+ Spec	0.81 (0.01)	0.89 (0.02)	0.80 (0.01)	0.80 (0.01)	0.90 (0.04)	0.79 (0.01)	0.78 (0.01)	0.91 (0.02)	0.77 (0.01)	0.41
MinROCdist	0.82 (0.01)	0.87 (0.03)	0.81 (0.01)	0.81 (0.01)	0.88 (0.04)	0.80 (0.01)	0.81 (0.01)	0.88 (0.02)	0.81 (0.01)	0.42
P. carpenteri										
Sens=Spec	0.88 (0.01)	0.88 (0.03)	0.88 (0.01)	0.89 (0.01)	0.89 (0.05)	0.89 (0.01)	0.88 (0.01)	0.88 (0.03)	0.88 (0.01)	0.37
MaxSens+ Spec	0.85 (0.01)	0.96 (0.02)	0.85 (0.01)	0.87 (0.01)	0.97 (0.02)	0.86 (0.01)	0.84 (0.01)	0.97 (0.01)	0.84 (0.01)	0.21
MinROCdist	0.87 (0.01)	0.94 (0.02)	0.86 (0.01)	0.89 (0.01)	0.93 (0.04)	0.89 (0.01)	0.87 (0.01)	0.93 (0.02)	0.86 (0.01)	0.31

Table 5: Area of predicted suitable habitat broken down into entire model extent, and model extent in UK and Irish jurisdictions. Percentage of predicted suitable habitat protected by the MPA and NEAFC Closure network used by Ross et al. (2015) for the purpose of comparison, also broken down by national MPAs and NEAFC Closures.

		***D. pertusum* reef**			***P. carpenteri***		
		Ross & Howell 2013 GEBCO Model	Ross *et al.* 2015 200m^2 Model	New Model	Ross & Howell 2013 GEBCO Model	Ross *et al.* 2015 200m^2 Model	New Model
Entire Model Extent	Predicted Suitable Habitat	185,240.25 km^2	30,106.10 km^2	4748.32 km^2	218,725.88 km^2	73,709.68 km^2	54,289.48 km^2
	Predicted Suitable Habitat within MPAs/NEAFC Closures	12.81%	20.00%	31.61%	1.29%	2.64%	6.62%
Model extent within UK Shelf Claim	Predicted Suitable Habitat	57,425.06 km^2	8,281.48 km^2	1,244.00 km^2	87,516.00 km^2	9,514.00 km^2	8,886.76 km^2
	Predicted	29.84%	56.00%	58.95%	2.60%	11.20%	25.23%

	Suitable Habitat within MPAs/NEAFC Closures						
Model extent within Irish Shelf Claim	Predicted Suitable Habitat	48,139.31 km^2	21,665.48 km^2	3,412.36km^2	49,343.63 km^2	63,525.96 km^2	43,936.44 km^2
	Predicted Suitable Habitat within MPAs/NEAFC Closures	13.67%	12.60%	21.65%	1.10%	1.39%	2.86%

Table 6: Area of predicted suitable habitat for *D. pertusum* reef and *P. carpenteri* broken down into entire model extent, and model extent in UK and Irish jurisdictions. Percentage of predicted suitable habitat protected by the most up to data MPA/NEAFC Closure network and the EU / UK 800m trawl ban, also broken down by nation.

		D. pertusum reef	*P. carpenteri*
Entire Model Extent	Predicted Suitable Habitat	4,748.32 km^2	54,289.48 km^2
	800m Trawl Ban	60.11%	100.00%
	2020 MPA/NEAFC Network	40.26%	11.45%
Model extent within UK Shelf Claim	Predicted Suitable Habitat	1,244.00 km^2	8,886.76 km^2
	800m Trawl Ban	48.74%	100.00%
	2020 MPA/NEAFC Network	83.64%	49.30%
Model extent within Ireland Shelf Claim	Predicted Suitable Habitat	3,412.36 km^2	43,936.44 km^2
	800m Trawl Ban	64.25%	100.00%

	2020 MPA/NEAFC Network	24.45%	3.79%

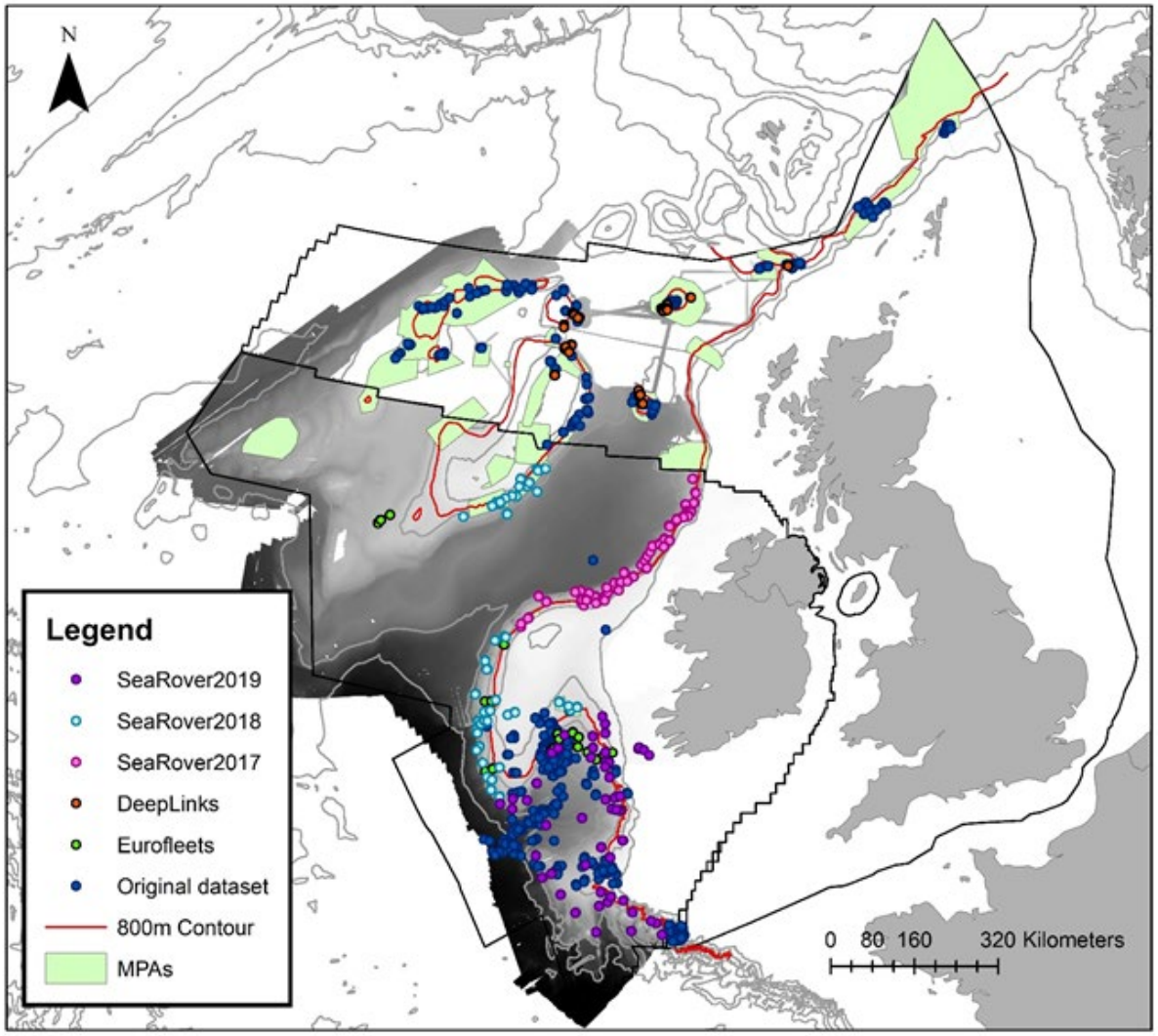

Figure 1: Map of the UK and Ireland's Continental Shelf Limits (black line) showing the original dataset from Ross & Howell (2013), and Ross et al. (2015) together with the new dataset (compiled from five different surveys over 5 years) used to independently validate the models and subsequently build new models. The current network of deep-sea Marine Protected Areas is shown, together with the 800m isobath, below which bottom trawling is prohibited. Bathymetry shown is the 200 x 200 m gridded multibeam dataset (see text below for detail) shaded for depth with contours of 200m, 500m, 1000m and intervals of 1000m thereafter shown in grey. Map projected in British National Grid for aesthetic reasons

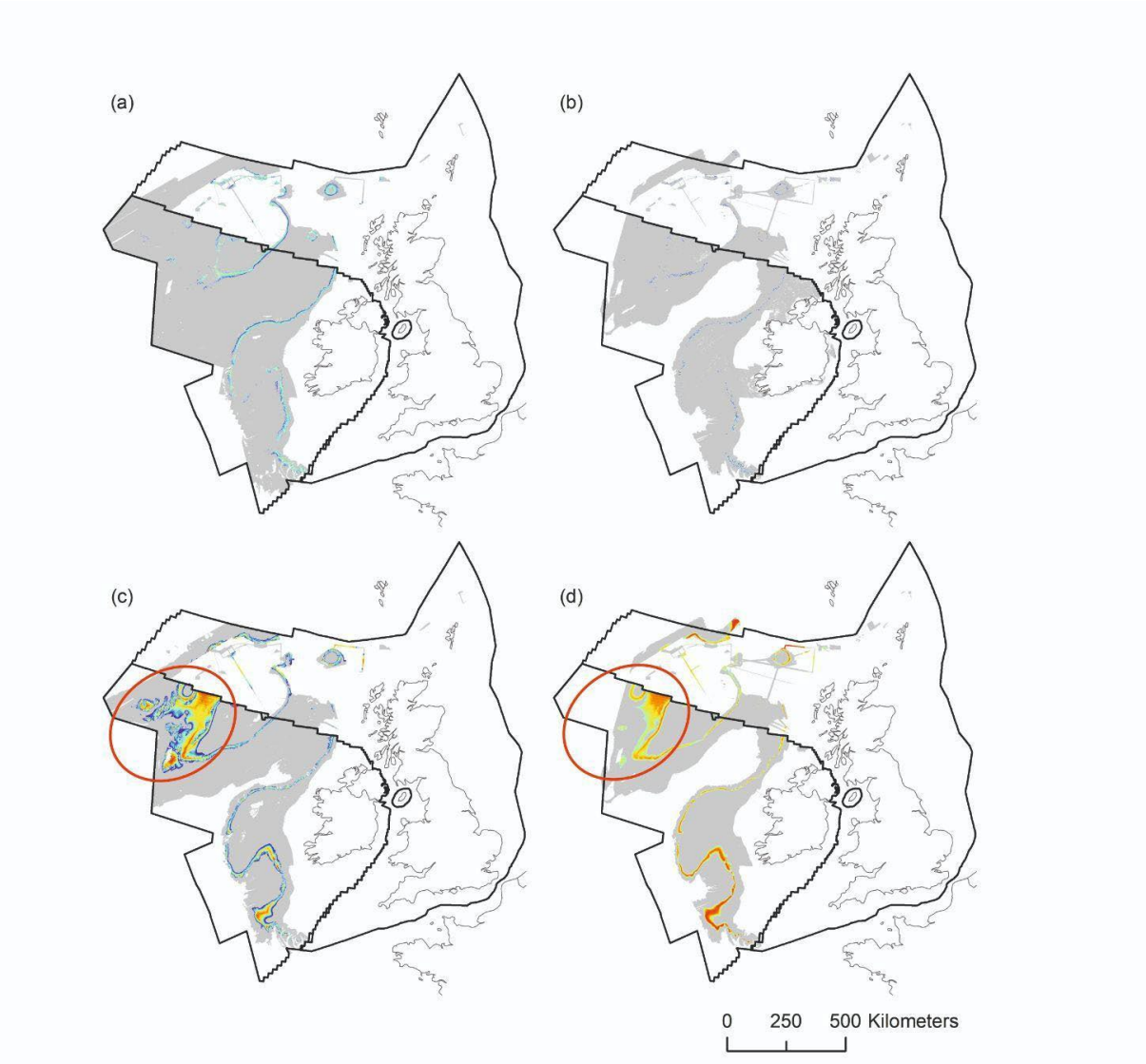

Figure 2: Above threshold full model prediction maps for: (a) scleractinian cold-water coral reef distribution from Ross *et al*. (2015); (b) *D. pertusum* reef distribution with the new dataset; (c) *P. carpenteri* aggregation distribution from Ross *et al*. (2015); (d) *P. carpenteri* aggregation distribution with the new dataset. The Hatton-Rockall Basin is circled in red in c and d. White background indicates the prediction has been masked for novel climates. Maps projected in British National Grid for aesthetic reasons.

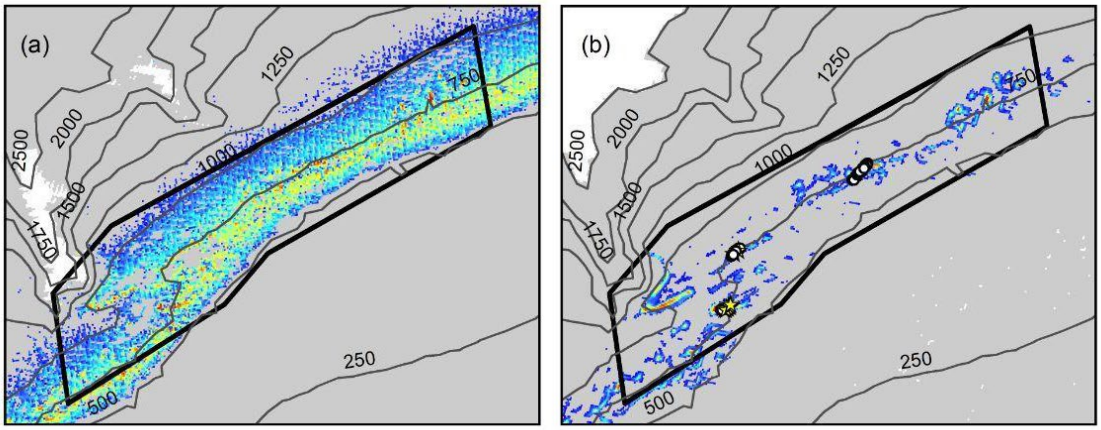

Figure 3: Examples of changes to protected area model predictions. (a) scleractinian cold-water coral reef distribution within the North-West Porcupine Bank MPA from Ross *et al*. (2015); (b) *D. pertusum* reef distribution within the North-West Porcupine Bank MPA with the new dataset. ROV transects plotted showing presences as yellow stars and absence as white circles. Maps projected in British National Grid for aesthetic reasons.